Tohoku J. Exp. Med., 2024, **263**, 151-160

New Dihydropyridine Derivative Attenuates NF-κB Activation via Suppression of Calcium Influx in a Mouse BV-2 Microglial Cell Line

Kota Sato,[1,2] Yuto Sasaki,[1] Michiko Ohno-Oishi,[1] Kuniyuki Kano,[3,*] Junken Aoki,[3,*] Kosuke Ohsawa,[3] Takayuki Doi,[3] Hiroyuki Yamakoshi,[3] Yoshiharu Iwabuchi,[3] Chihiro Kawano,[1] Yoshiyuki Hirata[4] and Toru Nakazawa[1,2,5,6]

[1]Department of Ophthalmology, Tohoku University Graduate School of Medicine, Sendai, Miyagi, Japan
[2]Department of Advanced Ophthalmic Medicine, Tohoku University Graduate School of Medicine, Sendai, Miyagi, Japan
[3]Graduate School of Pharmaceutical Sciences, Tohoku University, Sendai, Miyagi, Japan
[4]Faculty of Pharmacy, Osaka Medical and Pharmaceutical University, Takatsuki, Osaka, Japan
[5]Department of Retinal Disease Control, Tohoku University Graduate School of Medicine, Miyagi, Japan
[6]Department of Ophthalmic Imaging and Information Analytics, Tohoku University Graduate School of Medicine, Sendai, Miyagi, Japan

Activated microglia contribute to many neuroinflammatory diseases in the central nervous system. In this study, we attempted to identify an anti-inflammatory compound that could suppress microglial activation. We performed high-throughput screening with a chemical library developed at our institute. We performed a luciferase assay of nuclear factor-kappa B (NF-κB) reporter stable HT22 cells and identified a compound that was confirmed to inhibit the anti-inflammatory response in BV2 microglial cells. The selected dihydropyridine derivative can suppress the expression response of interleukin-1β (*IL-1β*), interleukin-6 (*IL-6*), and tumor necrosis factor (*TNF*), as well as NF-κB phosphorylation and nuclear translocation, and reduce the intracellular calcium level. Thus, our identified compound has a potential role in suppressing microglial activation and may contribute to the development of a new therapeutic molecule against neuroinflammatory diseases.

Keywords: dihydropyridine derivative; drug screening; inflammation; microglia
Tohoku J. Exp. Med., 2024 June, **263** (2), 151-160.
doi: 10.1620/tjem.2024.J024

Introduction

Retinal microglia in the eye have a role in the stages of normal development and also have a significant function in maintaining homeostasis in the mature retina. However, in pathological conditions, activated microglia are involved in neurodegenerative eye diseases, such as glaucoma, retinitis pigmentosa, and age-related neurodegeneration, because they produce proinflammatory neurotoxic cytokines (Silverman and Wong 2018; Rathnasamy et al. 2019). Glaucoma is a particularly important disease, being the leading cause of blindness worldwide, with the estimated number of patients expected to reach 100 million by the year 2040 (Tham et al. 2014). Glaucoma is characterized by optic neuropathy and the degeneration of retinal ganglion cells (RGCs) (Resnikoff et al. 2004). Optic nerve degeneration and visual loss in glaucoma is irreversible, making it the source of unmet medical needs. One therapeutic target is neuroinflammation caused by neurotoxic cytokines, which can directly injure RGCs and indirectly contribute to damage through RGCs (Tezel 2022).

The most important glaucoma risk factor is elevated intraocular pressure (IOP), which is a trigger for glial activation in the optic nerve head and retina (Kwon et al. 2009). In a model of acute glaucoma based on induced high IOP in the eyes of mice, the toll-like receptor 4 (TLR4)-mediated NLR family pyrin domain containing 1 (NLRP1)/NLR family pyrin domain containing 3 (NLRP3) inflammasome pathway and interleukin-1β (IL-1β) promoted RGC death (Chi et al. 2014). In our IOP-

Received November 26, 2023; revised and accepted March 23, 2024; J-STAGE Advance online publication April 4, 2024
*Present address: Graduate School of Pharmaceutical Sciences, The University of Tokyo, 7-3-1 Hongo, Bunkyo-ku, Tokyo 113-0033, Japan.
Correspondence: Toru Nakazawa, Department of Ophthalmology, Tohoku University Graduate School of Medicine, 1-1 Seiryo-machi, Aoba-ku, Sendai, Miyagi 980-8574, Japan.
e-mail: ntoru@oph.med.tohoku.ac.jp

independent optic nerve injury model, TLR4/Myd88 signaling was activated in the retinal microglia (Sato et al. 2023). Genetic studies have also revealed that multiple variants in the *TLR4* gene are associated with IOP-dependent and IOP-independent glaucoma (Shibuya et al. 2008; Takano et al. 2012; Navarro-Partida et al. 2017; Chen et al. 2019; Liu et al. 2020). This accumulation of evidence suggests that the retinal microglia contribute to pathological mechanisms by expressing inflammatory cytokines in glaucoma. Indeed, the intravitreal injection of tumor necrosis factor (TNF), a pathological cytokine in the retina, promotes optic nerve degeneration in the eyes of rats (Kitaoka et al. 2017). In addition, TNF secreted from microglia promotes astrocyte activation to a neurotoxic state A1, and these A1 astrocytes induce RGC loss via saturated lipids and their synthesized enzyme, termed elongation of very long-chain fatty acids protein 1 (ELOVL1) (Liddelow et al. 2017; Burda and Sofroniew 2017; Guttenplan et al. 2021). Recently, we also reported that retinal microglia are activated by optic nerve injury and that a subpopulation of G-protein coupled receptor 84 (GPR84)-positive microglia highly express TNF, while the deletion of GPR84-positive microglia attenuates RGC death in mice (Sato et al. 2023). These studies suggest that activated retinal microglia are a therapeutic target and that the suppression of an excessive inflammatory response related to the retinal microglia could be a therapeutic approach to treat glaucoma.

In this study, we tried to uncover an anti-nuclear factor-kappa B (NF-κB) inhibitor from the original chemical library of Tohoku University, which contains 6,080 unique compounds, with high throughput screening; a dihydropyridine derivative has the effect of suppressing inflammatory events by suppressing calcium influx in BV-2 cells in a microglial cell line. Thus, the compound that we identified may be a possible new therapeutic agent against eye diseases such as glaucoma that involve activated microglia.

Material and Methods

Cell culture, transfection, and test compounds

An HT22 cell line comprising mouse hippocampal neuronal cells was kindly provided as a gift by Prof. Yoko Hirata (Gifu University, Japan). The cells were cultured in Dulbecco's modified Eagle's medium (DMEM, 041-29775, FUJIFILM Wako Pure Chemical, Osaka, Japan) supplemented with 5% fetal bovine serum (FBS), 100 U/mL penicillin, and 100 μg/ml streptomycin (1% Pen/Strep, Gibco, 15140-122, Life Technologies, Waltham, MA, USA) at 37°C with 5% CO_2. To establish HT22 cells stably expressing the NF-κB reporter gene (HT22/NF-κB/luc), the cells were transfected with pGL4.32 [luc2P/NF-κB-RE/Hygro] (Promega, Madison, WI, USA) vector using lipofectamine 2000 transfection reagent (Thermo Fisher Scientific, Waltham, MA, USA). The stably transfected cells were selected with hygromycin B (400 μg/ml, Nacalai Tesque Inc., Kyoto, Japan) for two weeks. The 6,080 compounds were screened using a chemical library provided by the Department of Pharmacology, Tohoku University. Arctigenin was kindly provided by Dr. Yoshiyuki Hirata (Osaka Medical and Pharmaceutical University, Japan).

NF-κB reporter assay for first screening

To determine the effect of the compound on TNF-mediated activation of NF-κB, 1 μl/well of a stock chemical compound (200 μM) was plated in a 384-well plate. Next, the HT22/NF-κB/luc cells were seeded at a density of 2,000 cells/well, and 2 μl/well of TNFα (500 ng/ml) were incubated overnight. Luciferase activity was measured using the ONE-Glo luciferase assay system kit (Promega) according to the manufacturer's instructions. Luminescence was measured with a PHERAstar plate reader (BMG Labtech, Ortenberg, Baden-Württemberg, Germany). The relative luciferase activity of each group was compared to the control group.

Cell viability assay

To determine the effect of the compound on cell viability, HT22/NF-κB/luc and BV-2 cells were seeded at densities of 5,640 cells/well and 5,000 cells/well, respectively, and were incubated overnight in 96-well plates. The cells were pretreated with the compound for 6 hours. Alamar blue reagent (Invitrogen, Carlsbad, CA, USA) was added, and the fluorescence intensity was measured (at 560 nm excitation and 590 nm emission) with an absorption spectrometer (Vmax; Molecular Devices, San Jose, CA, USA) as previously described (Sato et al. 2021).

Cytotoxicity detection

To inspect the toxic effect of compound #38, we measured cell injury with a Cytotoxicity LDH Assay Kit (CK12, Dojindo Molecular Technologies, Kumamoto, Japan) and an Alamar blue assay (DAL1100, Thermo Fisher Scientific). BV2 cells from an immortalized mouse microglial cell line (Interlab Cell Line Collection, Genova, Italy) were incubated in a 96-well plate at a density of 5,000 cells/100 μl/well overnight and were added to 25 μl of compound #38 (2, 10, 50 μM) for 1 hour and 6 hours. Then, 62.5 μl of supernatant was moved to another well, and 62.5 μl of LDH was added for 30 minutes to measure the extent of cell death. Also, 6.25 μl of Alamar blue was added to the rest of the wells for 2 hours to measure the extent of cell survival.

Microglial cell culture and test compound

BV2 cells were cultured in DMEM with 5% FBS, 1% Pen/Strep in an incubator at 5% CO_2 and 37°C. In the experiments to examine the anti-inflammatory effect of compound #38, BV2 cells were pretreated with the compound for 1 hour and then treated with lipopolysaccharide (LPS; Sigma-Aldrich, St. Louis, MO, USA; 0.24 μg/ml) for 6 hours after BV2 cells were incubated in a 96-well plate overnight in DMEM (5% FBS, 1% Pen/Strep).

Quantitative PCR

BV2 cells were seeded at a density of 5,000 cells/well

in 100 μl DMEM and cultured in a 96-well plate overnight. They were then treated with compound #38 (2, 10, 50 μM) for 1 hour and LPS for 6 hours. Total RNA extraction and reverse transcription were conducted using the SuperPrep Cell Lysis and RT kit for qPCR (SCQ-401, Toyobo, Osaka, Japan) according to the manufacturer's protocol. Predesigned primers and probes purchased from Life Technology were used as follows, with the relevant genes in italics: *Il-1β* (Mm00434228_m1), *Il-6* (Mm00446100_m1), *Ccl2* (Mm00441242_m1), *Tnf-α* (Mm00443258_m1), *Gpr84* (Mm 02620530_s1) and *Gapdh* (Mm01256744_m1). The data were analyzed using the comparative Ct method (2-*ΔΔ*CT) and normalized to the control, *Gapdh*.

Immunocytochemistry

BV2 cells were seeded at a density of 25,000 cells/well in 500 μl DMEM and cultured in an 8-well slide chamber (S6815-1PAK, Nunc Lab-Tek II - CC2) overnight. They then received compound #38 treatment for 1 hour before LPS treatment for 6 or 24 hours. The cells were fixed in 4% paraformaldehyde at 4°C overnight. After washing with 0.05% Tween-20 in PBS (Tw-PBS), the cells were treated in 0.5% Triton X-100 in 0.05% Tw-PBS for 10 minutes to make the membrane transparent, blocked with 10% donkey serum (D9663, Sigma-Aldrich) in 0.05% Tw-PBS at room temperature for 1 hour, and incubated with anti-phospho-NF-κB antibody (1:200 dilution, 8242S, Cell Signaling Technology, Danvers, MA, USA) at room temperature for 1 hour. After washing with 0.05% Tw-PBS, the sections were incubated with Alexa Fluor 488 conjugated goat anti-rabbit IgG antibody (1:500 dilution, A21206, Invitrogen) or in blocking buffer at room temperature for 1 hour. Each section was mounted with ProLong Diamond Antifade Mountant with DAPI (P36962, Invitrogen). Representative fluorescence images were captured with BZ-X810 (Keyence, Osaka, Japan).

Immunoblot

BV2 cells were seeded at a density of 300,000 cells/well in 1 ml DMEM and cultured in a 6-well plate overnight; they then underwent compound #38 treatment for 1 hour before LPS treatment for 6 hours. After the BV2 cells were collected for PBS in a phosphatase inhibitor (04 906 845 001, Roche, Penzberg, Germany) and a protease inhibitor (5871S, New England Biolabs, Ipswtich, MA, USA), they were separated into the nuclear fraction with a kit (Nuclear/Cytosolic Fraction kit, AKR-171, Cell Biolabs, San Diego, CA, USA) according to the kit protocol. Total protein concentration was determined using the Pierce BCA Protein Assay Kit (23225, Thermo Fisher Scientific) and measured with a SpectraMax M2 (Molecular Devices). Protein from each sample was resolved by SDS-PAGE electrophoresis at 180 V for 30 minutes, after which the samples were transferred to membranes with a Trans-Blot Turbo (BIO-RAD, Hercules, CA, USA) and blocked with 1% skim milk at room temperature for 1 hour. Membranes were incubated with anti-NF-κB antibody (1:5,000 dilution, 3033S, Cell Signaling Technology) at room temperature for 1 hour. After washing with 0.05% Tw-PBS, the membranes were incubated with anti-rabbit HRP (1:5,000 dilution, A0545, Sigma-Aldrich) at room temperature for 1 hour. Next, the membranes were treated with ECL Prime western blotting detection reagents (RPN2232, GE Healthcare, Chicago, IL, USA) at room temperature for 5 minutes and captured by Chemi Doc XRS+ (BIO-RAD). After washing the membranes with WB stripping solution (05364-55, Nacalai Tesque Inc), anti-lamin B antibody (1:5,000 dilution, A21206, Invitrogen) was used as a loading control, and donkey anti-goat HRP (1:5,000 dilution, SAB3700284, Sigma-Aldrich) was used as a secondary antibody for loading control.

Calcium signal detection

BV2 cells were seeded at a density of 40,000 cells/well in 100 μl DMEM and cultured in a 96-well F-bottom Poly-D-Lysine black plate (655946, Greiner Bio-One, Stonehouse, Gloucestershire, UK) overnight. The cells were pretreated with 100 μl of 5 mM probenecid (p8761-25G, Sigma-Aldrich), which is used to prevent calcium from flowing out of cells, for 1 hour before being incubated with the FLIPR Calcium 5 Assay Kit for 1 hour according to the kit protocol. After that, compound #38 treatment (50 μM) was conducted for 1 hour. Measurement of intracellular Ca^{2+} levels in BV2 cells that underwent the above treatment was conducted simultaneously with LPS stimulation with a FlexStation 3 (Molecular Devices).

Statistical Analysis

All statistical comparisons were performed with a parametric one-way analysis of variance (ANOVA) using Prism9 software. Group differences were calculated with Dunnett's test among three or more groups. The significance level was set at $p < 0.05$.

Results

High-throughput screening to identify anti-inflammatory compounds by inhibiting NF-κB activation

First, we established an NF-κB reporter cell line to identify anti-inflammatory compounds from our chemical library. TNF stimulation can activate NF-κB in HT22 cells, and we evaluated the inhibitory response of NF-κB activation using 6,080 compounds. Using 10 μM of each compound, we defined the criterion for a hit as "a compound whose NF-κB activity is less than the mean –3 standard deviations (SDs) of all compounds." Thus, we used 58.76% as the criterion for NF-κB activity; as a result, 44 hit compounds were selected for the next step (Fig. 1). Second, we evaluated whether the effect on cell viability of NF-κB inhibition in the first screening was due to cytotoxicity. We re-examined the NF-κB activity using 10 μM of each compound, and determined cell viability with an Alamar blue assay. We used arctigenin as a positive control, as it can

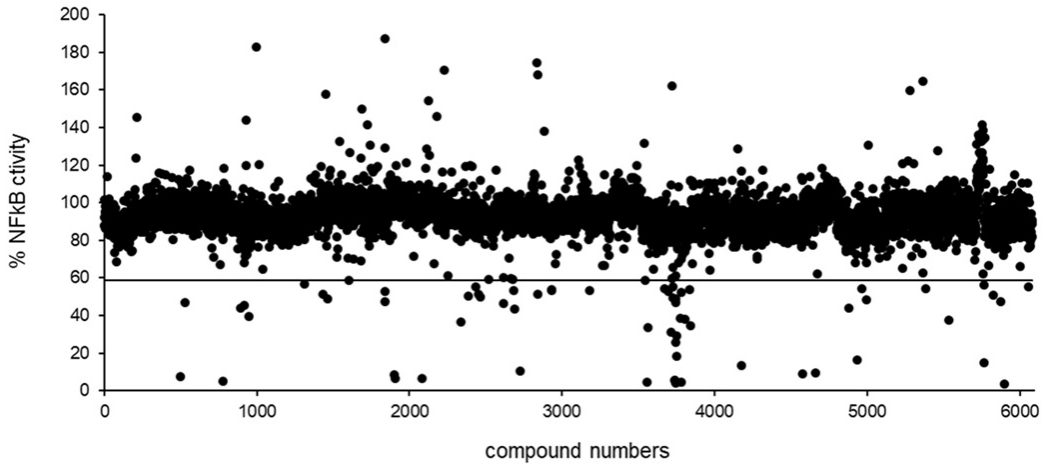

Fig. 1. First screening for the compound with a luciferase reporter gene assay.
The luciferase activity of the reporter genes in each compound was measured using a luciferase assay system and corrected using cells that were treated with 0.5% DMSO (v/v) as a control group. Each dot shows a compound, with a total of 6,080 compounds. Hit criteria were set up for each 384-well plate, and 44 hits were selected. The black line shows the hit criteria average across all plates (= 58.76%).

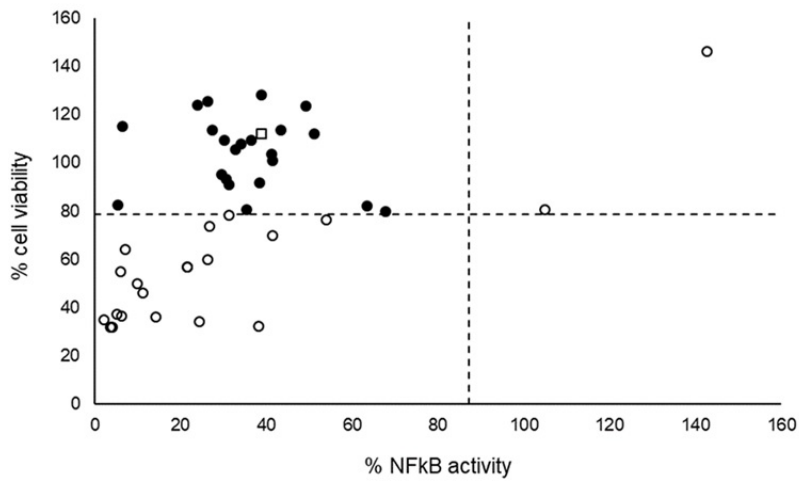

Fig. 2. Hit confirmation with the luciferase reporter gene and the Alamar blue assay.
The scatter plot shows a total of 44 compounds; 22 hit compounds were selected according to ≤ 87.3% NF-κB activity and ≥ 78.6% cell viability. The dotted line shows each hit criterion. Hits (black circles), non-hits (white circles), and 10 μM Arctigenin (ARC; white square) are also shown.

attenuate neuroinflammation by suppressing NF-κB translocation into nuclei and blocking cytokine expression (Xu et al. 2020). In the second screening, we set the criterion for a hit as "a compound whose NF-κB activity is less than the mean –3 SD of TNF-treated cells and a compound whose cell viability is more than the mean –3 SD of TNF-untreated cells." Arctigenin met the screening criteria that we set for NF-kB inhibition and low cell toxicity. We selected 22 hit compounds that had ≤ 87.3% NF-κB activity and ≥ 78.6% cell viability (Fig. 2). Third, we tested if different concentrations (0.1, 1, 10 50 μM) of the compound had a gradually increasing NF-κB inhibition effect in HT22 cells (Fig. 3, Supplementary Table S1). Arctigenin showed the ability to inhibit NF-kB activity in a dose-dependent manner, and showed no cell toxicity, even at a high dose. In this test, 4 compounds were selected as hits (#24, #26, #38, and #39) based on the following criteria: greater cell viability in the negative control (TNF-), i.e., mean –3 SD at a 1-μM dose of the compound, and less NF-κB activity in the positive control (TNF+), i.e., mean –3 SD at a 1-μM dose of the compound. Finally, we evaluated *Ccl2* expression to confirm the proinflammatory response against LPS-stimulated BV2 microglial cells (data not shown); we found that compound #38 was the best at suppressing microglial activation. Compound #38 has a dihydropyridine backbone (Fig. 4A). It has been also reported that even existing drugs that have dihydropyridine skeletons, such as nifedipine (Huang et al. 2014) and nicardipine, have the effect of suppressing

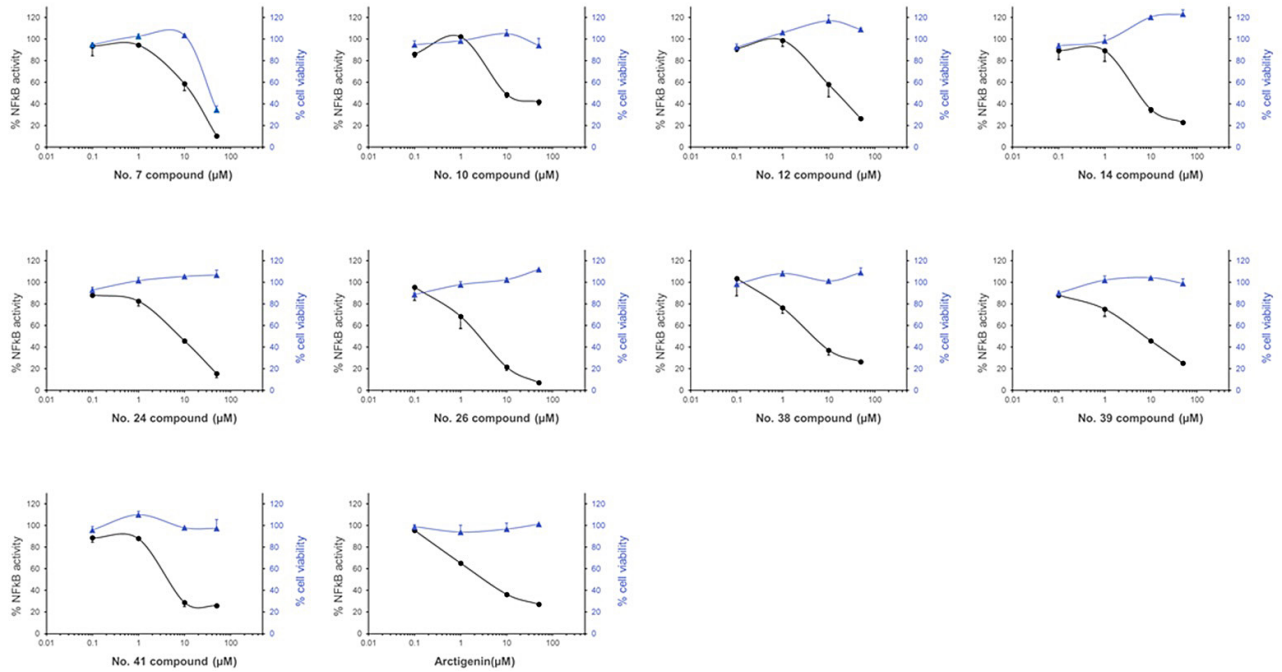

Fig. 3. The dose-dependent effect on NF-κB activity and cell viability of the candidate agents.
Each compound was assessed at four concentrations (0.1, 1, 10, 50 μM). NF-κB activity (black circles) and cell viability (blue triangles) are indicated. Error bars represent SDs (N = 2 for each concentration).

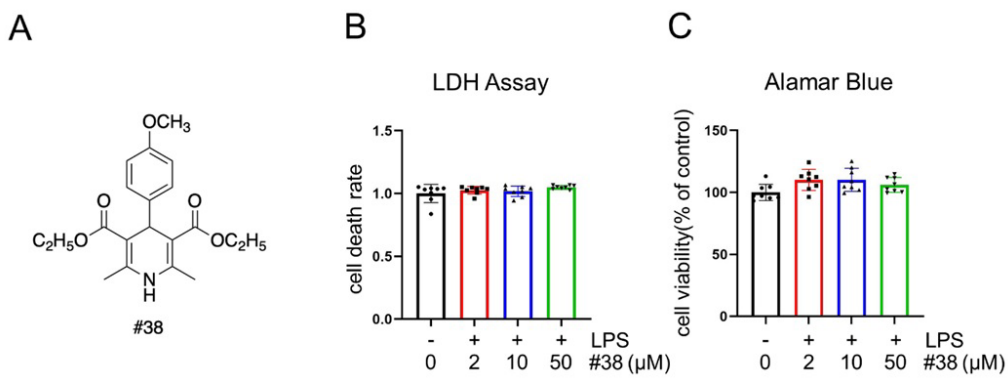

Fig. 4. Evaluation of the cytotoxicity of compound #38.
(A) Chemical structure of compound #38. Histogram showing cell death rate (B) and cell viability (C) assessed after treatment with compound #38 (0, 2, 10, 50 μM) for 60 min before application of LPS (0.24 μg/ml) for 6 h, represented as quantitative data from the cytotoxicity LDH assay and Alamar blue assay. This statistical analysis used Dunnett's test. The results are expressed as mean ± SD. N = 8.

microglial inflammation (Huang et al. 2014; Espinosa-Parrilla et al. 2015). Thus, we next evaluated the effect on the anti-inflammatory response and its mechanisms. First, to evaluate the cytotoxicity of compound #38, we conducted a cytotoxicity LDH assay and an Alamar blue assay. Even with treatment with 50 μM of compound #38, the cell death rate in the cytotoxicity LDH assay and cell viability in the Alamar blue assay did not significantly change; there was no cytotoxic effect in BV2 microglial cells (Fig. 4B, C).

Compound #38 suppressed mRNA expression of inflammatory mediators in LPS-stimulated BV-2 cell lines

Previous research reported that LPS stimulation increased the expression of inflammatory cytokines and chemokines (Puntambekar et al. 2011; Bao et al. 2019). To evaluate the anti-inflammatory effect of compound #38, we compared the expression of inflammatory cytokine mRNA at various concentrations (2, 10, 50 μM) of compound #38. We found that the expression of *Il-1β*, *Il-6*, and *Tnf-α* was elevated by LPS stimulation and suppressed by treatment with compound #38 in a dose-dependent manner (Fig. 5A-C). Moreover, compound #38 also reduced the expression of *Gpr84*, a marker of neurotoxic retinal microglia under LPS stimulation in BV-2 cells (Fig. 5D). These results indicate that compound #38 has anti-inflammatory effects in microglial cells and mostly suppresses the expres-

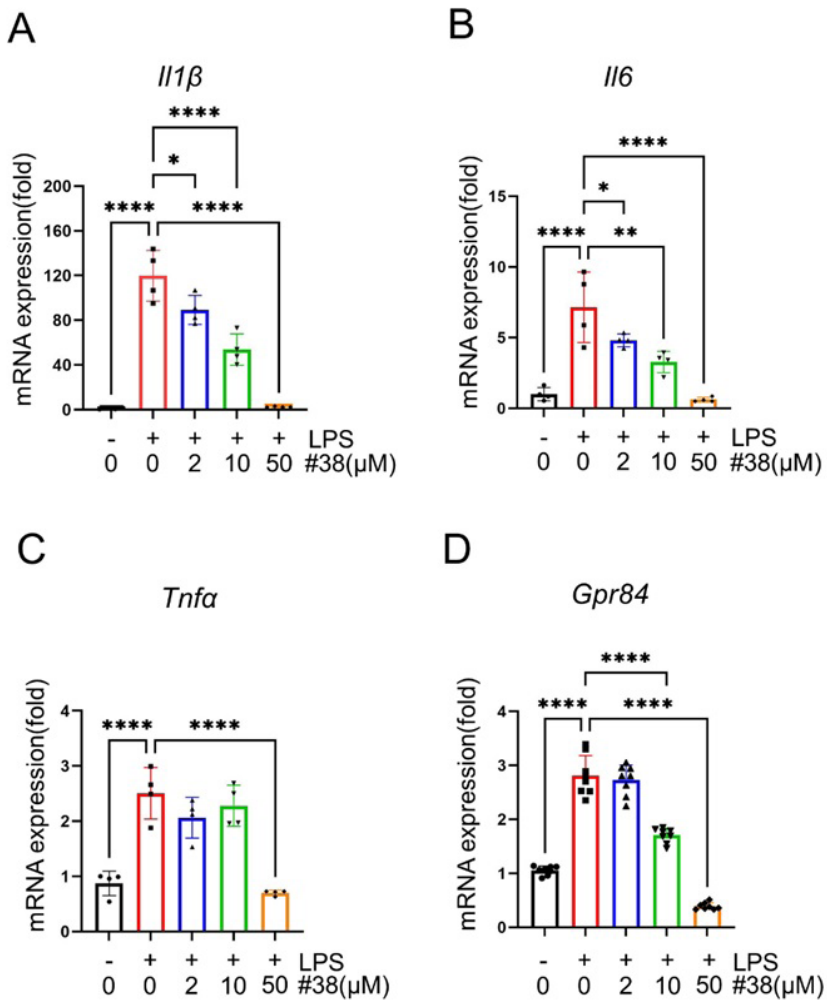

Fig. 5. Inhibitory effect of compound #38 on LPS-stimulated inflammatory mediators.
Transcriptional levels of *Il-1β* (A), *Il-6* (B), *Tnf-α* (C) and *Gpr84* (D) in BV2 cells pretreated with compound #38 (2, 10, 50 μM) for 1 h before application of LPS (0.2 μg/ml) for 6 h. This statistical analysis used Dunnett's test. The results are expressed as mean ± SD. N = 4-8, *p < 0.05, **p < 0.01, ****p < 0.0001.

sion of inflammatory cytokine mRNA at 50 μM.

Compound #38 suppressed NF-κB phosphorylation and nuclear translocation

To demonstrate the mechanism of compound #38's inhibition of the inflammatory response, we next examined whether compound #38 inhibited NF-κB phosphorylation and nuclear translocation. Previous research demonstrated that LPS stimulation may increase NF-κB phosphorylation and translocation (Li et al. 2019; Wu et al. 2020). Immunocytochemistry analysis showed that LPS increased NF-κB phosphorylation in BV2 cells, and pre-treatment with compound #38 suppressed LPS-induced NF-κB phosphorylation. Furthermore, as seen in Fig. 6A, it seems that compound #38 also suppressed NF-κB nuclear translocation. To quantitatively evaluate the extent of NF-κB nuclear translocation, we conducted an immunoblot analysis. The results showed that LPS increased NF-κB nuclear translocation in BV2 cells, and pre-treatment with compound #38 suppressed LPS-induced NF-κB nuclear translocation (Fig. 6B). We quantified the immunoblot results and summarized them in a graph. NF-κB nuclear translocation was significantly increased by LPS and suppressed by compound #38 (Fig. 6C). The results described above suggest that the anti-inflammatory effect of compound #38 is due to the suppression of NF-κB phosphorylation and nuclear translocation.

Compound #38 suppressed LPS-induced calcium changes

We further studied the mechanism of the anti-inflammatory effect of compound #38. We conducted experiments to determine the compound's effect on calcium influx, because it has a dihydropyridine skeleton that is expected to work as an L-type calcium channel blocker (Huang et al. 2014). It was previously reported that LPS stimulation increases the influx of calcium in BV2 cells because LPS stimulation activates the L-type calcium channel, which is largely expressed in microglia like BV2 (Saddala et al. 2020). We demonstrated that compound #38

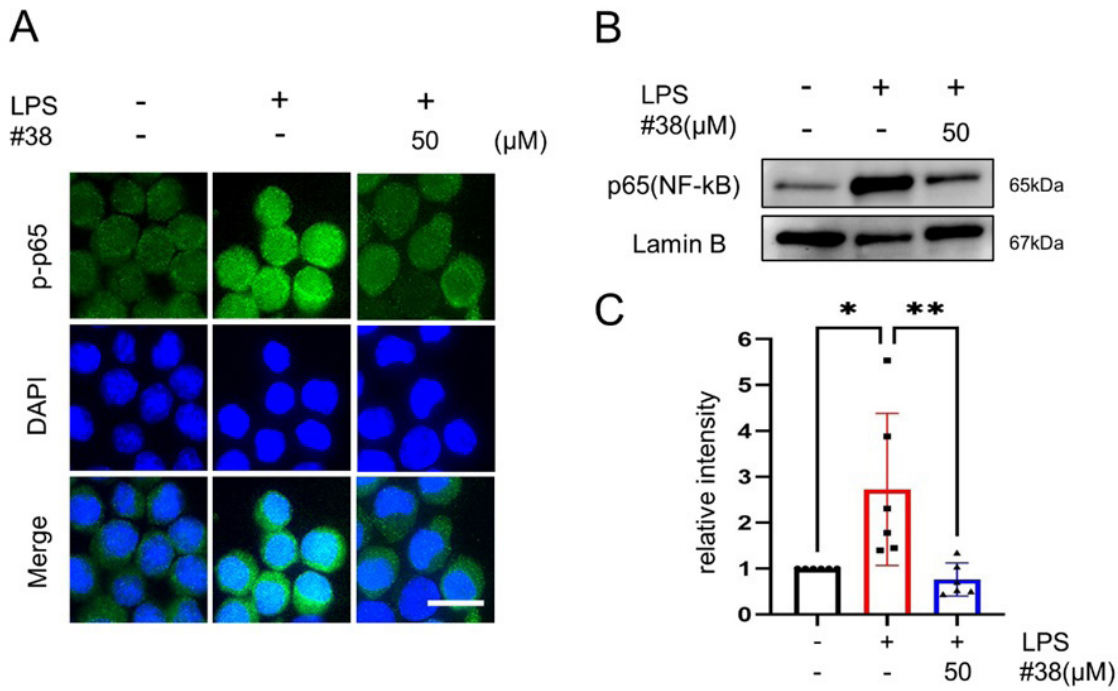

Fig. 6. Suppressive effect of compound #38 on NF-κB nuclear translocation and phosphorylation.
(A) Representative immunofluorescence images showing the distribution of p-NF-κB after treatment with compound #38 (50 μM) for 1 h and LPS (0.2 μg/ml) for 6 h. Scale bar is equal to 20 μm. Immunoblot images (B) and histogram (C) for NF-κB in the nuclear fraction after treatment with compound #38 (50 μM) for 1 h and LPS (0.2 μg/ml) for 6 h. This statistical analysis used Dunnett's test. The results are expressed as mean ± SD. N = 6, *p < 0.05, **p < 0.01.

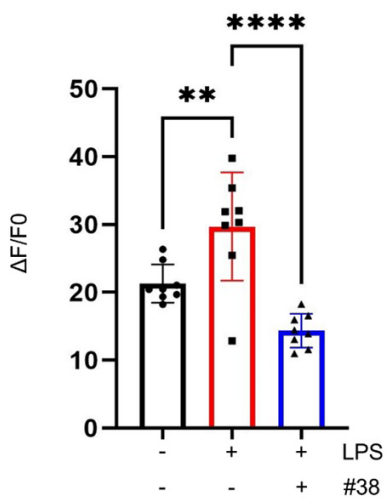

Fig. 7. Inhibitory effect of compound #38 on LPS-induced calcium influx.
The histogram shows calcium influx in BV2 cells assessed after treatment with compound #38 (50 μM) and the FLIPR Calcium 5 Assay Kit and probenecid. Measurement of calcium influx in BV2 cells was conducted simultaneously with LPS stimulation (0.2 μg/ml). This statistical analysis used Dunnett's test. The results are expressed as mean ± SD. N = 8, **p < 0.01, ****p < 0.0001.

suppresses LPS-induced calcium influx. We found that calcium influx in BV2 cells was significantly increased by LPS stimulation, and this LPS-induced calcium influx was significantly suppressed by treatment with compound #38 (Fig. 7).

Discussion

Microglia play important roles in combating infection, clearing cellular debris, maintaining tissue homeostasis, and contributing to progress of neurodevelopmental programs (Cowan and Petri 2018; Prinz et al. 2019). On the other hand, hyperactivation of microglia results in increasing production of proinflammatory mediators that may cause neurodegenerative diseases (Hickman et al. 2018), including Alzheimer's disease (Hansen et al. 2018; Rajendran and Paolicelli 2018), Huntington's disease (Palpagama et al. 2019), Parkinson's disease (George et al. 2019), prion disease (Carroll and Chesebro 2019). Reactive microglia are associated not only with brain diseases, but also eye diseases such as uveitis (Okunuki et al. 2019; Yuan et al. 2019), photoreceptor degeneration in retinal detachment (Wang et al. 2021), diabetic retinopathy (Hu et al. 2022), and glaucoma (Ishikawa et al. 2023). In such diseases, the central nervous system becomes a highly steroidogenic environment that synthesizes steroids, and it also metabolizes steroids deriving from the circulation (Yilmaz et al. 2019). In addition to steroid production in the body, the use of steroid medication suppresses neuroinflammation.

However, in individuals susceptible to steroids, steroids can cause a clinical condition similar to primary open-angle glaucoma. Once this disease occurs, surgery and gene therapy may be needed (Razeghinejad and Katz 2012). Therefore, non-steroidal anti-inflammatory medicine for the microglia is needed. Compound #38, which was screened in this experiment, does not have a steroidal skeleton, but rather a dihydropyridine skeleton. Thus, compound #38 can be used as an anti-neuroinflammation drug even in patients who have neuroinflammatory disease and are steroid responders.

Dihydropyridines are broadly used to block L-type voltage-dependent Ca^{2+} channels (L-VDCCs) and protect against cardiovascular diseases (Hopp 2021). Currently, dihydropyridines are also being examined for use in several central nervous system diseases. For example, intracellular Ca^{2+} and cytokine production were found to be elevated in cultured microglia stimulated with amyloid β or prion proteins, and these events were blocked by nifedipine, a type of dihydropyridine (Silei et al. 1999). In fact, activated microglia express L-VDCCs *in vivo*, and their L-VDCCs are functionally associated with cytokine release and the phagocytic capacity of BV2 cells *in vitro* (Espinosa-Parrilla et al. 2015). LPS, a ligand for TLR4, is a well-known activator that promotes pro-inflammatory cytokine release from microglia, and it is suppressed by Ca^{2+} chelators or indirect blockade of Ca^{2+} entry, suggesting that Ca^{2+} is an essential regulator of microglial phenotypes (Hoffmann et al. 2003; Dolga et al. 2012). Nimodipine, a kind of dihydropyridine used as an L-VDCC blocker, inhibits the production of pro-inflammatory cytokines such as TNF and IL-1β in LPS-stimulated microglia (Li et al. 2009). Details of the mechanism by which the L-VDCCs are regulated in LPS-stimulated microglia are still unclear; however, the accumulated evidence mentioned above demonstrates that Ca^{2+} influx in LPS-stimulated microglia is involved with L-VDCC opening, which supports our current results.

Cytosolic Ca^{2+} modulates intracellular signaling with calcium binding proteins such as adaptor molecule 1, calmodulin, and calcineurin (Hopp 2021). In particular, the inflammatory state of the microglia is regulated by nuclear factor of activated T cells (NFAT) via calcineurin binding with Ca^{2+} (Kurland et al. 2016). Rising intracellular calcium concentration also causes NF-κB phosphorylation and nuclear translocation (Huang et al. 2014; Saddala et al. 2020). Phosphorylated NF-κB in the nucleus promotes the transcription of inflammatory cytokine mRNA and activates the microglia, which causes neuroinflammation (Lipscombe et al. 2004; Madore et al. 2020). Compounds that have a dihydropyridine skeleton, such as compound #38, suppress L-VDCC opening (Gao and Yan 2021). Overall, compound #38 showed an anti-inflammatory effect by suppressing LPS-induced L-VDCC opening, reducing the influx of calcium, constricting the phosphorylation and nuclear translocation of NF-κB, and restraining the release of inflammatory substances. In addition to extracellular Ca^{2+} influx, intracellular Ca^{2+} regulation is also important for regulating microglial phenotypes. It is well known that the endoplasmic reticulum (ER) has an important role in Ca^{2+} storage and regulates Ca^{2+} levels in cells. Ryanodine receptors (RyRs) regulate Ca^{2+} release from the ER, and RyR antagonists can rescue microglia from the neurotoxic phenotype under LPS stimulation (Klegeris et al. 2007). Past studies also demonstrate that not only L-VDCCs, but also intracellular signaling receptors, such as the inositol trisphosphate receptors and RyRs, are also important targets to prevent microglial activation.

Our previous study demonstrated that retinal microglia are activated during RGC death in several models of retinal damage, such as ischemia/reperfusion, excitotoxicity, and optic nerve crush (Sato et al. 2020a, 2021, 2023). Compound #38 in particular can suppress the elevation of Gpr84, which we newly identified as a marker of neurotoxic retinal microglia expressing TNF/IL-1α. We recently reported that deleting *GPR84* in mice attenuated RGC death in an IOP-independent glaucoma model (Sato et al. 2023). We previously developed a drug delivery system (DDS) to continuously release drugs for RGC protection in rats that received optic nerve injury (Sato et al. 2020b). DDSs such as our newly developed device may help compound #38 effectively and continuously reach the RGCs. An experiment to investigate this will be needed in the future.

In conclusion, calcium channel blockers like compound #38 can be useful as a treatment for various inflammatory diseases involving the microglia. Therefore, the results of this screening study, which revealed compound #38 as a valid hit, show that we were able to discover a new substance with anti-inflammatory effects against microglia.

Acknowledgments

We thank Yoko Hirata (Gifu University, Japan) for generously providing the mouse HT22 hippocampal cells. We also thank Mr. Tim Hilts for editing this document, and Mr. Seiya Mochida, Ms. Junko Sato, Ms. Rieko Kamii, and Ms. Yurika Nakagawa for technical assistance. We also thank the Biomedical Research Unit of Tohoku University Hospital for technical support. Selected artwork in the graphical abstract were used pictures provided by Servier Medical Art (Servier; https://smart.servier.com/), licensed under a Creative Commons Attribution 4.0 Unported License. This research was partially supported by the Platform Project for Supporting Drug Discovery and Life Science Research (Basis for Supporting Innovative Drug Discovery and Life Science Research; BINDS) from AMED under grant numbers JP21am0101095 and JP22ama121040. This work was also supported in part by JST (grant number JPMJPF2201).

Conflict of Interest

The authors declare no conflict of interest.

References

Bao, Y., Zhu, Y., He, G., Ni, H., Liu, C., Ma, L., Zhang, L. & Shi, D. (2019) Dexmedetomidine Attenuates Neuroinflammation In LPS-Stimulated BV2 Microglia Cells Through Upregulation Of miR-340. *Drug Des. Devel. Ther.*, **13**, 3465-3475.

Burda, J.E. & Sofroniew, M.V. (2017) Seducing astrocytes to the dark side. *Cell Res.*, **27**, 726-727.

Carroll, J.A. & Chesebro, B. (2019) Neuroinflammation, Microglia, and Cell-Association during Prion Disease. *Viruses*, **11**, 65

Chen, M., Yu, X., Xu, J., Ma, J., Chen, X., Chen, B., Gu, Y. & Wang, K. (2019) Association of Gene Polymorphisms With Primary Open Angle Glaucoma: A Systematic Review and Meta-Analysis. *Invest. Ophthalmol. Vis. Sci.*, **60**, 1105-1121.

Chi, W., Li, F., Chen, H., Wang, Y., Zhu, Y., Yang, X., Zhu, J., Wu, F., Ouyang, H., Ge, J., Weinreb, R.N., Zhang, K. & Zhuo, Y. (2014) Caspase-8 promotes NLRP1/NLRP3 inflammasome activation and IL-1beta production in acute glaucoma. *Proc. Natl. Acad. Sci. U. S. A.*, **111**, 11181-11186.

Cowan, M. & Petri, W.A. Jr. (2018) Microglia: Immune Regulators of Neurodevelopment. *Front. Immunol.*, **9**, 2576.

Dolga, A.M., Letsche, T., Gold, M., Doti, N., Bacher, M., Chiamvimonvat, N., Dodel, R. & Culmsee, C. (2012) Activation of KCNN3/SK3/K(Ca)2.3 channels attenuates enhanced calcium influx and inflammatory cytokine production in activated microglia. *Glia*, **60**, 2050-2064.

Espinosa-Parrilla, J.F., Martinez-Moreno, M., Gasull, X., Mahy, N. & Rodriguez, M.J. (2015) The L-type voltage-gated calcium channel modulates microglial pro-inflammatory activity. *Mol. Cell. Neurosci.*, **64**, 104-115.

Gao, S. & Yan, N. (2021) Structural Basis of the Modulation of the Voltage-Gated Calcium Ion Channel Ca(v) 1.1 by Dihydropyridine Compounds*. *Angew. Chem. Int. Ed. Engl.*, **60**, 3131-3137.

George, S., Rey, N.L., Tyson, T., Esquibel, C., Meyerdirk, L., Schulz, E., Pierce, S., Burmeister, A.R., Madaj, Z., Steiner, J.A., Escobar Galvis, M.L., Brundin, L. & Brundin, P. (2019) Microglia affect alpha-synuclein cell-to-cell transfer in a mouse model of Parkinson's disease. *Mol. Neurodegener.*, **14**, 34.

Guttenplan, K.A., Weigel, M.K., Prakash, P., Wijewardhane, P.R., Hasel, P., Rufen-Blanchette, U., Munch, A.E., Blum, J.A., Fine, J., Neal, M.C., Bruce, K.D., Gitler, A.D., Chopra, G., Liddelow, S.A. & Barres, B.A. (2021) Neurotoxic reactive astrocytes induce cell death via saturated lipids. *Nature*, **599**, 102-107.

Hansen, D.V., Hanson, J.E. & Sheng, M. (2018) Microglia in Alzheimer's disease. *J. Cell Biol.*, **217**, 459-472.

Hickman, S., Izzy, S., Sen, P., Morsett, L. & El Khoury, J. (2018) Microglia in neurodegeneration. *Nat. Neurosci.*, **21**, 1359-1369.

Hoffmann, A., Kann, O., Ohlemeyer, C., Hanisch, U.K. & Kettenmann, H. (2003) Elevation of basal intracellular calcium as a central element in the activation of brain macrophages (microglia): suppression of receptor-evoked calcium signaling and control of release function. *J. Neurosci.*, **23**, 4410-4419.

Hopp, S.C. (2021) Targeting microglia L-type voltage-dependent calcium channels for the treatment of central nervous system disorders. *J. Neurosci. Res.*, **99**, 141-162.

Hu, Z., Mao, X., Chen, M., Wu, X., Zhu, T., Liu, Y., Zhang, Z., Fan, W., Xie, P., Yuan, S. & Liu, Q. (2022) Single-Cell Transcriptomics Reveals Novel Role of Microglia in Fibrovascular Membrane of Proliferative Diabetic Retinopathy. *Diabetes*, **71**, 762-773.

Huang, B.R., Chang, P.C., Yeh, W.L., Lee, C.H., Tsai, C.F., Lin, C., Lin, H.Y., Liu, Y.S., Wu, C.Y., Ko, P.Y., Huang, S.S., Hsu, H.C. & Lu, D.Y. (2014) Anti-neuroinflammatory effects of the calcium channel blocker nicardipine on microglial cells: implications for neuroprotection. *PLoS One*, **9**, e91167.

Ishikawa, M., Izumi, Y., Sato, K., Sato, T., Zorumski, C. F., Kunikata, H. & Nakazawa, T. (2023) Glaucoma and microglia-induced neuroinflammation. *Frontiers in Ophthalmology*, **3**, 1–8.

Kitaoka, Y., Sase, K., Tsukahara, C., Kojima, K., Shiono, A., Kogo, J., Tokuda, N. & Takagi, H. (2017) Axonal Protection by Ripasudil, a Rho Kinase Inhibitor, via Modulating Autophagy in TNF-Induced Optic Nerve Degeneration. *Invest. Ophthalmol. Vis. Sci.*, **58**, 5056-5064.

Klegeris, A., Choi, H.B., McLarnon, J.G. & McGeer, P.L. (2007) Functional ryanodine receptors are expressed by human microglia and THP-1 cells: Their possible involvement in modulation of neurotoxicity. *J. Neurosci. Res.*, **85**, 2207-2215.

Kurland, D.B., Gerzanich, V., Karimy, J.K., Woo, S.K., Vennekens, R., Freichel, M., Nilius, B., Bryan, J. & Simard, J.M. (2016) The Sur1-Trpm4 channel regulates NOS2 transcription in TLR4-activated microglia. *J. Neuroinflammation*, **13**, 130.

Kwon, Y.H., Fingert, J.H., Kuehn, M.H. & Alward, W.L. (2009) Primary open-angle glaucoma. *N Engl J Med*, **360**, 1113-1124.

Li, C., Zhao, B., Lin, C., Gong, Z. & An, X. (2019) TREM2 inhibits inflammatory responses in mouse microglia by suppressing the PI3K/NF-kappaB signaling. *Cell Biol. Int.*, **43**, 360-372.

Li, Y., Hu, X., Liu, Y., Bao, Y. & An, L. (2009) Nimodipine protects dopaminergic neurons against inflammation-mediated degeneration through inhibition of microglial activation. *Neuropharmacology*, **56**, 580-589.

Liddelow, S.A., Guttenplan, K.A., Clarke, L.E., Bennett, F.C., Bohlen, C.J., Schirmer, L., Bennett, M.L., Munch, A.E., Chung, W.S., Peterson, T.C., Wilton, D.K., Frouin, A., Napier, B.A., Panicker, N., Kumar, M., et al. (2017) Neurotoxic reactive astrocytes are induced by activated microglia. *Nature*, **541**, 481-487.

Lipscombe, D., Helton, T.D. & Xu, W. (2004) L-type calcium channels: the low down. *J. Neurophysiol.*, **92**, 2633-2641.

Liu, H., Qi, S., He, W., Chang, C., Chen, Y. & Yu, J. (2020) Association of single-nucleotide polymorphisms in TLR4 gene and gene-environment interaction with primary open angle glaucoma in a Chinese northern population. *J. Gene Med.*, **22**, e3139.

Madore, C., Yin, Z., Leibowitz, J. & Butovsky, O. (2020) Microglia, Lifestyle Stress, and Neurodegeneration. *Immunity*, **52**, 222-240.

Navarro-Partida, J., Martinez-Rizo, A.B., Ramirez-Barrera, P., Velazquez-Fernandez, J.B., Mondragon-Jaimes, V.A., Santos-Garcia, A. & Benites-Godinez, V. (2017) Association of Toll-like receptor 4 single-nucleotide polymorphisms Asp299Gly and Thr399Ile with the risk of primary open angle glaucoma. *Graefes Arch. Clin. Exp. Ophthalmol.*, **255**, 995-1001.

Okunuki, Y., Mukai, R., Nakao, T., Tabor, S.J., Butovsky, O., Dana, R., Ksander, B.R. & Connor, K.M. (2019) Retinal microglia initiate neuroinflammation in ocular autoimmunity. *Proc. Natl. Acad. Sci. U. S. A.*, **116**, 9989-9998.

Palpagama, T.H., Waldvogel, H.J., Faull, R.L.M. & Kwakowsky, A. (2019) The Role of Microglia and Astrocytes in Huntington's Disease. *Front. Mol. Neurosci.*, **12**, 258.

Prinz, M., Jung, S. & Priller, J. (2019) Microglia Biology: One Century of Evolving Concepts. *Cell*, **179**, 292-311.

Puntambekar, S.S., Davis, D.S., Hawel, L. 3rd, Crane, J., Byus, C.V. & Carson, M.J. (2011) LPS-induced CCL2 expression and macrophage influx into the murine central nervous system is polyamine-dependent. *Brain. Behav. Immun.*, **25**, 629-639.

Rajendran, L. & Paolicelli, R.C. (2018) Microglia-Mediated Synapse Loss in Alzheimer's Disease. *J. Neurosci.*, **38**, 2911-2919.

Rathnasamy, G., Foulds, W.S., Ling, E.A. & Kaur, C. (2019)

Retinal microglia - A key player in healthy and diseased retina. *Prog. Neurobiol.*, **173**, 18-40.
Razeghinejad, M.R. & Katz, L.J. (2012) Steroid-induced iatrogenic glaucoma. *Ophthalmic Res.*, **47**, 66-80.
Resnikoff, S., Pascolini, D., Etya'ale, D., Kocur, I., Pararajasegaram, R., Pokharel, G.P. & Mariotti, S.P. (2004) Global data on visual impairment in the year 2002. *Bull World Health Organ*, **82**, 844-851.
Saddala, M.S., Lennikov, A., Mukwaya, A., Yang, Y., Hill, M.A., Lagali, N. & Huang, H. (2020) Discovery of novel L-type voltage-gated calcium channel blockers and application for the prevention of inflammation and angiogenesis. *J. Neuroinflammation*, **17**, 132.
Sato, K., Mochida, S., Tomimoto, D., Konuma, T., Kiyota, N., Tsuda, S., Shiga, Y., Omodaka, K. & Nakazawa, T. (2020a) A pyruvate dehydrogenase kinase inhibitor prevents retinal cell death and improves energy metabolism in rat retinas after ischemia/reperfusion injury. *Exp. Eye Res.*, **193**, 107997.
Sato, K., Nakagawa, Y., Omodaka, K., Asada, H., Fujii, S., Masaki, K. & Nakazawa, T. (2020b) The Sustained Release of Tafluprost with a Drug Delivery System Prevents the Axonal Injury-induced Loss of Retinal Ganglion Cells in Rats. *Curr. Eye Res.*, **45**, 1114-1123.
Sato, K., Ohno-Oishi, M., Yoshida, M., Sato, T., Aizawa, T., Sasaki, Y., Maekawa, S., Ishikawa, M., Omodaka, K., Kawano, C., Ohue-Kitano, R., Kimura, I. & Nakazawa, T. (2023) The GPR84 molecule is a mediator of a subpopulation of retinal microglia that promote TNF/IL-1alpha expression via the rho-ROCK pathway after optic nerve injury. *Glia*, **71**, 2609-2622.
Sato, K., Sato, T., Ohno-Oishi, M., Ozawa, M., Maekawa, S., Shiga, Y., Yabana, T., Yasuda, M., Himori, N., Omodaka, K., Fujita, K., Nishiguchi, K.M., Ge, S. & Nakazawa, T. (2021) CHOP deletion and anti-neuroinflammation treatment with hesperidin synergistically attenuate NMDA retinal injury in mice. *Exp. Eye Res.*, **213**, 108826.
Shibuya, E., Meguro, A., Ota, M., Kashiwagi, K., Mabuchi, F., Iijima, H., Kawase, K., Yamamoto, T., Nakamura, M., Negi, A., Sagara, T., Nishida, T., Inatani, M., Tanihara, H., Aihara, M., et al. (2008) Association of Toll-like receptor 4 gene polymorphisms with normal tension glaucoma. *Invest. Ophthalmol. Vis. Sci.*, **49**, 4453-4457.
Silei, V., Fabrizi, C., Venturini, G., Salmona, M., Bugiani, O., Tagliavini, F. & Lauro, G.M. (1999) Activation of microglial cells by PrP and beta-amyloid fragments raises intracellular calcium through L-type voltage sensitive calcium channels. *Brain Res.*, **818**, 168-170.
Silverman, S.M. & Wong, W.T. (2018) Microglia in the Retina: Roles in Development, Maturity, and Disease. *Annu. Rev. Vis. Sci.*, **4**, 45-77.
Takano, Y., Shi, D., Shimizu, A., Funayama, T., Mashima, Y., Yasuda, N., Fukuchi, T., Abe, H., Ideta, H., Zheng, X., Shiraishi, A., Ohashi, Y., Nishida, K., Nakazawa, T. & Fuse, N. (2012) Association of Toll-like receptor 4 gene polymorphisms in Japanese subjects with primary open-angle, normal-tension, and exfoliation glaucoma. *Am. J. Ophthalmol.*, **154**, 825-832 e821.
Tezel, G. (2022) Molecular regulation of neuroinflammation in glaucoma: Current knowledge and the ongoing search for new treatment targets. *Prog. Retin. Eye Res.*, **87**, 100998.
Tham, Y.C., Li, X., Wong, T.Y., Quigley, H.A., Aung, T. & Cheng, C.Y. (2014) Global prevalence of glaucoma and projections of glaucoma burden through 2040: a systematic review and meta-analysis. *Ophthalmology*, **121**, 2081-2090.
Wang, Y., Zhao, X., Gao, M., Wan, X., Guo, Y., Qu, Y., Chen, Y., Li, T., Liu, H., Jiang, M., Wang, F. & Sun, X. (2021) Myosin 1f-mediated activation of microglia contributes to the photoreceptor degeneration in a mouse model of retinal detachment. *Cell Death Dis.*, **12**, 926.
Wu, S.Y., Pan, B.S., Tsai, S.F., Chiang, Y.T., Huang, B.M., Mo, F.E. & Kuo, Y.M. (2020) BDNF reverses aging-related microglial activation. *J. Neuroinflammation*, **17**, 210.
Xu, X., Piao, H.N., Aosai, F., Zeng, X.Y., Cheng, J.H., Cui, Y.X., Li, J., Ma, J., Piao, H.R., Jin, X. & Piao, L.X. (2020) Arctigenin protects against depression by inhibiting microglial activation and neuroinflammation via HMGB1/TLR4/NF-kappaB and TNF-alpha/TNFR1/NF-kappaB pathways. *Br. J. Pharmacol.*, **177**, 5224-5245.
Yilmaz, C., Karali, K., Fodelianaki, G., Gravanis, A., Chavakis, T., Charalampopoulos, I. & Alexaki, V.I. (2019) Neurosteroids as regulators of neuroinflammation. *Front. Neuroendocrinol.*, **55**, 100788.
Yuan, Z., Chen, X., Yang, W., Lou, B., Ye, N. & Liu, Y. (2019) The anti-inflammatory effect of minocycline on endotoxin-induced uveitis and retinal inflammation in rats. *Mol. Vis.*, **25**, 359-372.

Supplementary Files

Please find supplementary file(s);
https://doi.org/10.1620/tjem.2024.J024